ELSEVIER

Journal of Alloys and Compounds 439 (2007) 279–286

Journal of ALLOYS AND COMPOUNDS

www.elsevier.com/locate/jallcom

Microstructure and high-temperature wear and oxidation resistance of laser clad γ/W_2C/TiC composite coatings on γ-TiAl intermetallic alloy

Xiu-Bo Liu [a,b,*], Rong-Li Yu [c]

[a] *Laboratory for Laser Intelligent Manufacturing, Institute of Mechanics, Chinese Academy of Sciences, 15 Beisihuanxi Road, Beijing 100080, PR China*

[b] *School of Materials & Chemical Engineering, Zhongyuan Institute of Technology, 41 Zhongyuan Western Road, Zhengzhou 450007, Henan Province, PR China*

[c] *School of Materials Science and Engineering, Beihang University, 37 Xueyuan Road, Beijing 100083, PR China*

Received 30 June 2006; received in revised form 14 August 2006; accepted 20 August 2006
Available online 20 September 2006

Abstract

There are very strong interests in improving the high-temperature wear resistance of the γ-TiAl intermetallic alloy, especially when applied as tribological moving components. In this paper, microstructure, high-temperature dry sliding wear at 600 °C and isothermal oxidation at 1000 °C on ambient air of laser clad γ/W_2C/TiC composite coatings with different constitution of Ni–Cr–W–C precursor mixed powders on TiAl alloy substrates have been investigated. The results show that microstructure of the laser fabricated composite coatings possess non-equilibrium microstructure consisting of the matrix of nickel-base solid solution γ-NiCrAl and reinforcements of TiC, W_2C and $M_{23}C_6$ carbides. Higher wear resistance than the original TiAl alloy is achieved in the composite coatings under high-temperature wear test conditions. However, the oxidation resistance of the laser clad γ/W_2C/TiC composite coatings is deceased. The corresponding mechanisms resulting in the above behaviors of the laser clad composite coatings are discussed.

Keywords: γ-TiAl intermetallic alloy; γ/W_2C/TiC composite coatings; High-temperature wear resistance; Laser cladding

1. Introduction

Because of its high strength-to-weight ratio, superior specific modulus and excellent high-temperature creep resistance, γ-TiAl intermetallic alloy (hereafter referred as TiAl alloy) has great potential in elevated temperature structural applications. [1–3]. Recently, significant efforts have been made on improving the room-temperature ductility and high-temperature oxidation resistance by alloy modifications, processing innovation and surface engineering [4–6]. Some advanced TiAl alloys are now nearly maturing to the stage where it is possible to implement them in industrial applications. But its usage is also limited due to the poor surface hardness (HV320) and wear resistance, especially high-temperature wear resistance, when TiAl alloy acting as elevated-temperature moving components (as high as 900 °C), for example turbine blades, in which tribological properties are critically important to the components service life. Laser surface technology is preliminary verified to be an effective and economical method to solve the high-temperature wear problem, especially under the conditions of large loads and severe mechanical stress [7]. In our previous study [8], the efforts of fabricating both wear and high-temperature oxidation resistant ceramic/cermet composite coatings on TiAl alloy with different constitution of NiCr–Cr_3C_2 precursor mixed powders were made, the results show that it is a promising surface modification technique for TiAl alloy when applied as high as 1000 °C.

Apart from high hardness, reinforced carbides WC (including W_2C, et al. tungsten carbides) has a unique set of properties, which includes high melting point, a low coefficient of thermal expansion, good plasticity and wettability by molten metals [9], that is why it is a well-known engineering material widely used for cutting and wear resistance applications. TiC is also widely

* Corresponding author. Tel.: +86 10 62651165; fax: +86 10 62521859.
E-mail address: liubobo0828@yahoo.com.cn (X.-B. Liu).

0925-8388/$ – see front matter © 2006 Elsevier B.V. All rights reserved.
doi:10.1016/j.jallcom.2006.08.065

used as the reinforced phase in composite materials owing to its high hardness, high modulus and rather high flexural strength [10]. So, both WC and TiC could act as reinforcing wear resistant phases due to their strong atomic bonds and good abrasive and erosive wear resistance and certain oxidation resistance in the composite coating materials. Simultaneously, there should exist continuous phase to play the critical role of firmly connecting and supporting the wear resistant phases so as to fully exert the wear resistant capabilities of the reinforced phases. The continuous phase should exhibit good combination properties including excellent high-temperature stability, oxidation-resistance and good toughness. This is because high-temperature structure stability and oxidation-resistance are prerequisites of the high-temperature coatings. As for good toughness, on the one hand, it could prevent cracking or delamination of the coatings during the high-temperature wear process and on the other hand, it could relieve the thermal stress during fabrication process. γ-austenitic solid solution is well known for its ductility and toughness, heat- and corrosion-resistant capabilities due to its compact face-centered-cubic crystal structure and supersaturation strengthening ability during the laser and other high energy beam induced non-equilibrium rapid melting and subsequent solidification process. It seems reasonable that γ austenitic solid solution matrix composite coatings reinforced by W_2C and TiC carbides are expected to possess good service properties under high-temperature and wear conditions.

The present study is to explore the feasibility of fabricating high-temperature wear resistant cermet composite coatings on TiAl alloys using Ni–Cr–W–C mixed powders by laser cladding, which is commonly used in conventional thermal spraying conditions to improve the wear resistance usually below 600 °C. Emphasis is placed on characterizing the microstructure and the evolution process of the laser clad composite coatings and investigating the high-temperature wear and oxidation behaviors. The aim is to enlarge the application scope of Ni–Cr–W–C mixed powders and the corresponding laser surface modification on TiAl alloy.

2. Experimental procedures

The starting experimental material was a commercial titanium aluminide alloy Ti–48Al–2Cr–2Nb (at. %). The TiAl alloy was melted using high purity charge materials by a vacuum magnetic-suspension induction skull-melting furnace (l00 kW). After repeated melting for three times, each time for 15 min, ingots, 40 mm in diameter and 180 mm in length, were cast. The as-cast ingots vacuum-sealed in quartz tube were homogenized at 1360 °C for 2 h to produce a fully lamellar microstructure. Specimens, with the size of 8 mm × 10 mm × 40 mm for laser cladding, were cut from the cast and homogenized ingots by electric discharging machine.

Experiments of laser cladding of the TiAl alloy were conducted on a 5 kW CO_2 laser materials processing systems with four-axes computer-numerical-controlled (CNC) working station. Specimens were first sandblasted and then cleaned with ethyl alcohol and acetone and painted with black paint to increase the laser-materials absorption before laser cladding. Mixed elemental powders of different constitution of Ni–Cr–W–C alloy, in proportion (vol. %) of 16:4:40:40, 40:10:25:25, 64:16:10:10, respectively, were mixed and bounded with cellulose aether and then pre-placed on the specimen's surface in thickness of about 1.5 mm. All the specimens were heated on a carbon steel hot-plate heated by a 2 kW electric stove to be adequately dried before laser beam irradiation, the particle size of the precursor powders ranged from 70–140 μm The purity of the above powders was about 98.0%. The laser cladding parameters were: laser output power 3.0 kW, beam diameter 5.0 mm, beam traverse speed 3.3 mm/s. Since the aim of this experiment is only exploration, the composite coatings were created by a single track for simpleness of subsequent analyses. Two steel blocks were placed tightly at two sides of each TiAl alloy specimen to absorb partial laser irradiated energy so as to avoid the marginal effect and possible plasma effect. A 4 L min^{-1} flow of argon gas was passed through the melt pool to provide a protective environment for the sake of avoiding the reaction between the molten metals and oxygen.

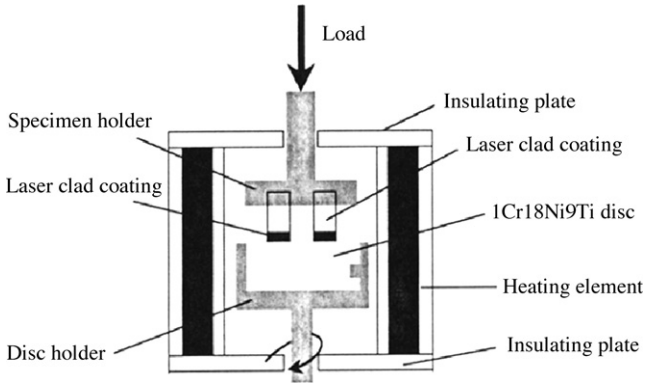

Fig. 1. Schematic illustration of the high-temperature dry sliding wear tester.

Metallographic samples and wear testing specimens were machined by electric discharging cutting, followed by mechanical milling and grinding to acquire the wear testing surface with roughness of 0.8 μm from the slight rough as-laser clad specimens. Metallographic samples of the composite coatings were prepared using standard mechanical polishing procedures and were etched in $HF:HNO_3:H_2O$ water solution in volume ratio of 1:6:7. Microstructure of the coatings was characterized by optical microscopy (OM), scanning electron microscopy (SEM) and energy-dispersive spectrometer (EDS). The phases present in the surface layer were identified by X-ray diffraction (XRD) using Cu Kα radiation. The recorded intensities and peak positions were compared with Joint Committee on Powder Diffraction Standards (JCPDS) data. The hardness profile along the coating depth was measured using a microhardness tester with a load of 2.94 N and a dwelling time of 15 s.

The high-temperature dry sliding wear test was carried out on a MMG-200 pin-on-disk wear testing machine as shown schematically in Fig. 1. To meet the dimension requirements of the tester, the original TiAl alloy and all the laser clad composite coatings were cut into 5 mm × 6 mm × 7 mm small blocks and used as the upper specimen with the 5 mm × 6 mm surface as the worn surface. The holder of the upper specimen was designed and manufactured by the authors. The lower specimen was a disc and the material was selected as a hot-rolled and solution-treated austenitic stainless steel 1Cr18Ni9Ti because of its relatively high hardness (HV430 at room-temperature) and good oxidation-resistance under high-temperature exposure. Specifications of the high-temperature wear tests were as follows: rotating speed of the principal axis was 100 rpm and resulted in the sliding speed of 0.1026 m/s, the load was 80 N, room-temperature running time was 20 min, high-temperature wear test cycle was 30 min. The tests are repeated three times. The wear weight loss was measured using a high accuracy photoelectric balance. The relative wear-resistance (i.e., the ratio of wear weight loss of the original specimen to that of the laser clad specimen) was utilized to judge the wear resistance.

In order to examine the elevated-temperature oxidation resistance of the laser clad composite coatings and the original alloys, isothermal oxidation was performed in a conventional high-temperature resistance furnace at 1000 °C for 50 h. The weight gains were measured using a high accuracy photoelectric balance and the relative high-temperature oxidation resistance (i.e., the ratio of oxidation weight gain per square millimeter of the original specimen to that of the laser clad specimen) was also used to rank the oxidation resistance.

SEM was used to characterize the worn surface and oxide scales formed on the surface of the laser clad composite coatings and original TiAl alloy to assist in analyzing the high-temperature wear and oxidation mechanisms.

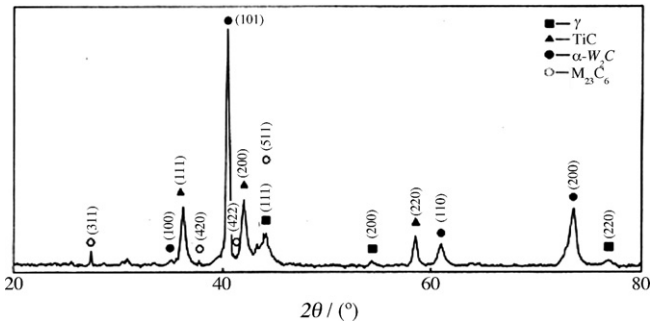

Fig. 2. XRD spectra of the laser clad γ/W_2C/TiC composite coating on TiAl alloy with Ni40Cr10W25C25 precursor mixed powders.

3. Results and discussion

3.1. Microstructure

As a result of the direct laser beam radiation, most of the precursor mixed Ni–Cr–W–C powders was melted onto the surface of the TiAl specimen with certain dilution of the substrate. After the forward moving of the laser beam and the subsequent non-equilibrium solidification of the melted bath which was highly supersaturated by chromium, carbon and some titanium and aluminium atoms, an in situ wear-resistant composite coating mainly reinforced by very hard tungsten carbide (W_2C) and titanium carbide (TiC) had been produced on the TiAl substrate, as indicated by XRD analysis results in Fig. 2.

Fig. 3 shows the transverse OM overview photomicrographs of the laser clad composite coating with precursor mixed powders of Ni40Cr10W25C25 and Ni64Cr16W10C10, respectively. It could be found that the surface of the laser clad composite coating with Ni40Cr10W25C25 was rough and there existed some round pores near the transition zone (as indicated by the arrows in Fig. 3a). Formation of these pores was mainly attributed to the super heating state of the laser induced alloying molten pool, WC particles were oxidized, burned and gave out large quantity of gas. Meanwhile, although shielding gas was used, the coating was oxidized, part of the engulfed ambient air was dissolved into the molten pool. The aforementioned gas did not have enough time to release owing to the subsequent rapid solidification. This phenomenon agrees well with the results of other authors [11]. No shrinkage cavities were found in the region between the substrate and the cladding, implying the suitable parameters applied in this sample, although it is another cause of porosity in pre-placed clad due to the lack of substrate material. A high-quality composite coating without porosity or cracking was obtained with Ni64Cr16W10C10 pre-placed mixed powders (as can be seen from Fig. 3b). As for the specimen pre-placed with Nil6Cr4W40C40, no integrate composite coating was formed due to the incompletely dissolution of the WC powders and inadequately intermixing with the substrate resulted from the relatively lower laser power and higher scan-speed, non-continuous liquid-drop shape clad layer was formed due to the action of surface tension during the cooling process and was detached completely during the metallographic specimen preparation. So, only the other two specimens underwent the microstructure and properties examination.

Typical microstructure of the laser clad composite coating on TiAl alloy with Ni64Cr16W10C10 precursor mixed powders can be seen in Fig. 4(a) and more clearly in Fig. 4(b), which is a high magnification SEM photograph showing the typical microstructures in the upper region of the composite coating. It can be seen that except for the continuous matrix, there are three main phases in the coating, the grey dendritic phase, white irregular blocky phase and the net-like phase precipitated along the grain boundary. Further EDS analysis indicates that the grey dendritic phase is carbide and enriched in Ti, the white irregular blocky phase contains large quantity of W and C, while the net-like phase is a compound enriched in Ni, Cr, Ti and C. Taking the XRD analysis results into account, it can be deduced that the laser clad layer is mainly composed of γ-NiCrAl matrix, TiC, tungsten carbides and chromium carbide or chromium and titanium composite carbide. It can be known from the W–C binary phase diagram that there exist three eutectic reactions, including three intermediate phase: W_2C, WC and α-WC_{1-x}. W_2C has polycrystalline transformation under high-temperature, i.e., there exists β-W_2C form between 2100 and 2400 °C and α-W_2C form below that temperature. Cottrell [12] calculated the reaction formation energy transformation between WC and W_2C under the C enriched and W enriched environments, which indicated that WC was preferentially formed under the C enriched environment and W_2C was relatively more stable under the W enriched or C depleted environment. So, it can be reasonably deduced that W_2C type carbides could be more preferentially formed during the C depleted laser molten pool. Because the

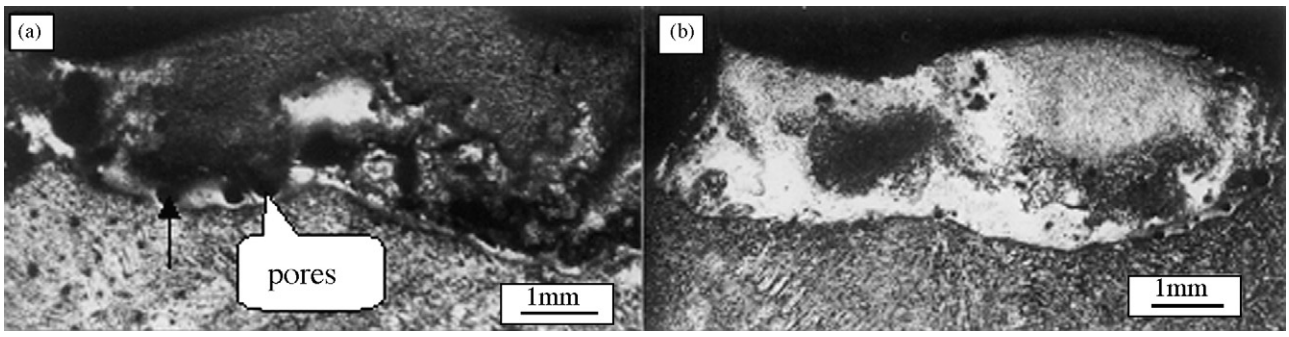

Fig. 3. Macrostructure of the laser clad composite coatings on TiAl alloy with (a) Ni40Cr10W25C25 and (b) Ni64Cr16Wl0C10 precursor mixed powders.

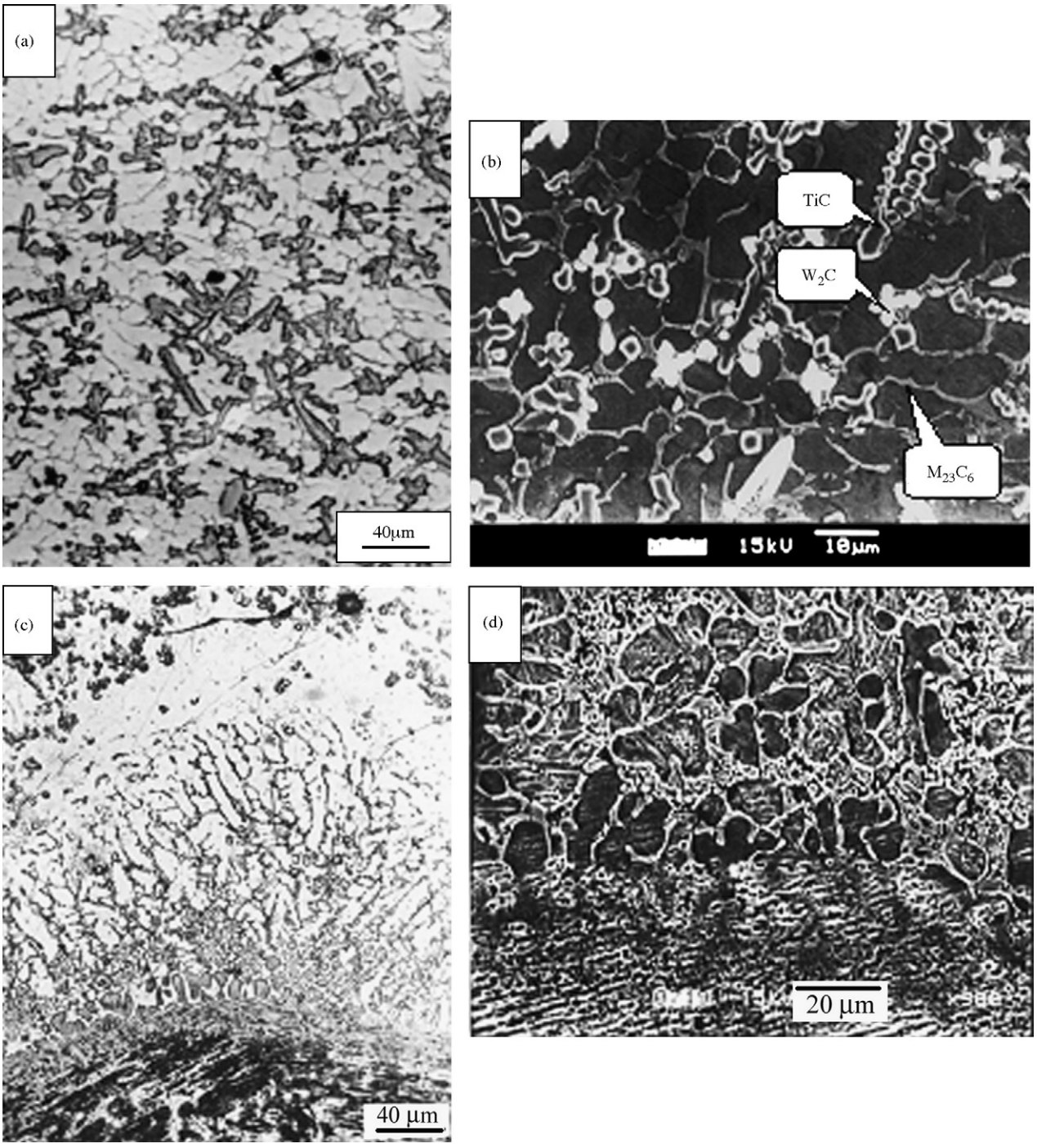

Fig. 4. Typical microstructure of the laser clad composite coating on TiAl alloy with Ni64Cr16W10C10 precursor mixed powders, (a) OM and (b) SEM photographs showing the non-equilibrium solidified W_2C, TiC and $M_{23}C_6$ phases uniformly distributed in the γ-NiCrAl matrix in the upper region, (c) OM and (d) SEM micrographs showing the pure metallurgical bonding to the substrate.

Gibbs energy formation of TiC (−184 kJ/mol) is very lower than that of the WC (−24.5 kJ/mol), plusing much higher melting point of TiC, titanium carbide precipitates preferably in the Ni–Cr–W–C–Ti–Al alloy system in the molten pool, resulting in certain depleted C environment. According to the above deduction, the subsequently precipitated tungsten carbide should be α-W_2C type. The polycrystalline transformation of these carbides often makes some metastable structure resulting from "freezing" owing to the rapid solidification. Chromium also has large affinity with C (the heat formation energy of Cr_7C_3 and $Cr_{23}C_6$ are −26.0 and −18.4 kJ/mol, respectively). Part of it is super-saturated in the γ solid solution, while the residual precipitated as $M_{23}C_6$ and mainly distributed along the grain boundary owing to the last solidification, in which $M_{23}C_6$ is $(Cr, Ti)_{23}C_6$ compound carbide with Ti atoms partly replaced Cr atoms.

It is interesting to note that both W_2C and TiC phases show uniform distribution in the whole coating. This phenomenon is different from other authors' results [13], which indicated that

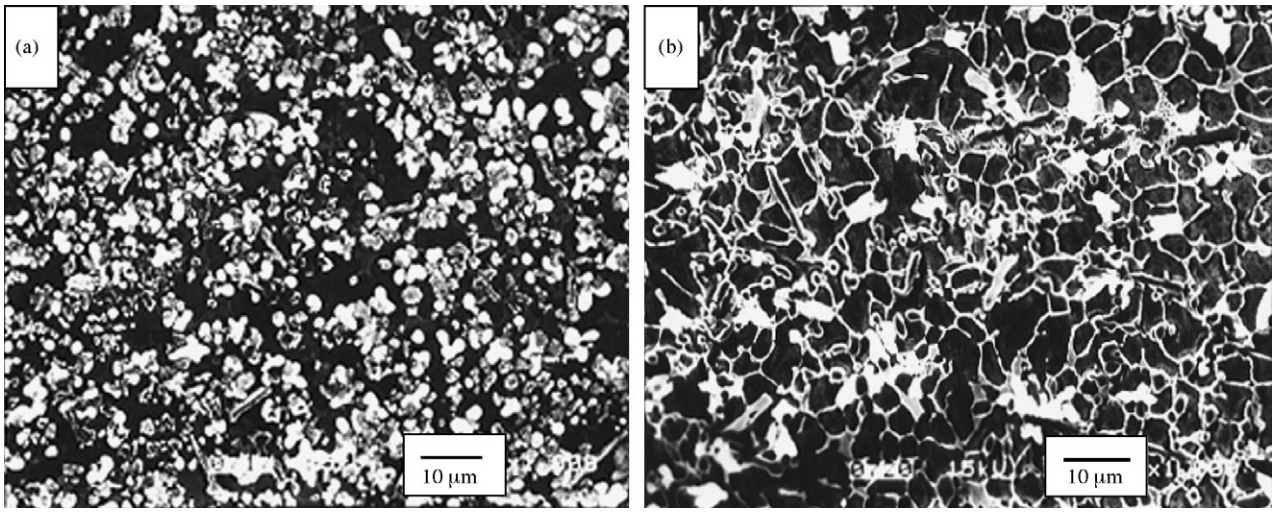

Fig. 5. SEM images showing the microstructure comparison of the laser clad composite coatings with (a) Ni40Cr10W25C25 and (b) Ni64Cr16W10C10 precursor mixed powders.

WC particles tend to sink to the lower region of the molten pool due to its higher density. In the present case, we propose that the stirring motion in the melting pool and the Marangoni convection for mixing the pre-placed particles was effective.

It can be found from Fig. 4(c and d) that a thin planar-front solidified layer epitaxially grew from the substrate. From the bonding zone to the central region and finally to the region near the surface of the laser clad composite coating, the whole microstructure shows gradient characteristics. The strong metallurgical interface between the coating and the substrate ensured excellent bonding strength and show high potentiality for enhancing wear resistance. Fig. 5 are the SEM images comparison of the central regions of the laser clad composite coating with Ni40Cr10W25C25 and Ni64Cr16W10C10 precursor mixed powders. It can be seen there exists no evidently microstructure difference between them. However, the volume fraction of the white irregular blocky phase (α-W_2C) and the grey granular or dendritic phase (TiC) of the composite coating with Ni64Cr16W10C10 was significantly lower than that of composite coating with Ni40Cr10W25C25. This implies that volume fraction of the reinforcement phases depends on the constitution of the precursor mixed powders to a great extent.

3.2. Microhardness and high-temperature sliding wear behavior

Because of the non-equilibrium solidified microstructure and the presence of large amount of hard primary W_2C and TiC carbides distributed in the γ matrix, it is anticipated by nature that the microhardness of the laser clad γ/W_2C/TiC composite coating would be improved significantly as compared to the TiAl substrate. Moreover, the microhardness of the laser clad composite coatings increased obviously in company with the increasing content of WC in the pre-placed mixed powders. The average hardness of the clad coating with Ni40Cr10W25C25 is higher (about HV900) than that with Ni64Cr16W10C10 (about HV600). This result agrees very well with the corresponding higher volume fraction of reinforcements of α-W_2C, TiC and $M_{23}C_6$, as can be seen in Fig. 5.

Results of the high-temperature sliding wear test show that wear weight loss of the Ni40Cr10W25C25 and Ni64Cr16W10C10 coating is 2 and 1.5 times lower than that of the original TiAl alloy, respectively. Fig. 6(a) shows the high-temperature worn surface morphology of the original TiAl alloy, both wide and deep ploughing grooves are visible on the worn surface. Based on the research results of Hawk and Alman [14], due to the inherent long-range ordered superstructure and the fairly good atomic bonding, all of the titanium–aluminide compounds (such as Ti_3Al, TiAl and Al_3Ti) possess similar wear rates and are more resistant to metallic adhesion than pure Ti and Ti-based alloys. So, it is relatively harder to improve the wear resistance of TiAl alloy than Ti-based alloys, in which case, the conventional sliding wear resistance can be enhanced as much as more than one hundred multiples. But on the other hand, the microhardness of TiAl alloy (HV320) is much lower than that of counterpart (HV430), these hard asperities can easily penetrate into the sliding surface of TiAl alloy. It implies that the mating counterpart has generated serious ploughing and scratching action on the original TiAl alloy under the wear temperature of 600 °C. EDS analysis of the left raised area shows the higher content of Fe, Cr, Ni and certain content of Ti and Al, which means that the adhesive transfer of the counterpart steel occurred under high temperature condition. Furthermore, some detached TiAl alloy wear debris are contained in the adhesive transfer layer based on EDS analysis, which implies the sliding surface of the original TiAl alloy is easy to be plastically deformed and plowed under high-temperature sliding wear test conditions, leading to the delamination and detachment of some wear debris. The composition of the grey granule in the right area of Fig. 6(a) is approaching 1Cr18Ni9Ti, which indicates that it is formed by the adhesive transfer action of the wear debris resulted from the micro-cutting of the mating counterpart steel. All the above analysis indicates that the dominant high-temperature sliding wear mechanisms of the original TiAl alloy

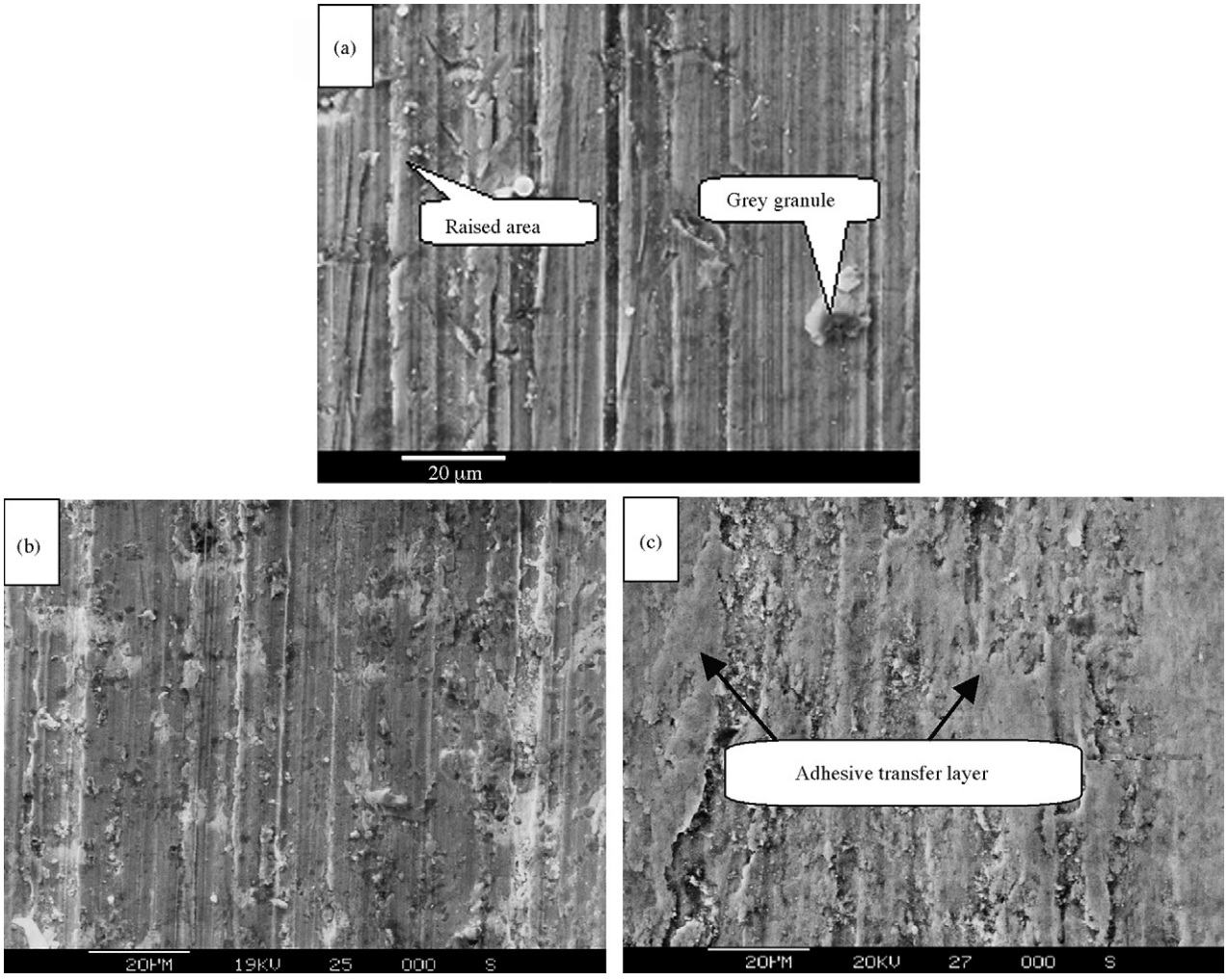

Fig. 6. SEM micrographs showing the high-temperature (600 °C) worn surfaces of (a) the original TiAl alloy and the laser clad composite coatings with (b) Ni40Cr10W25C25 and (c) Ni64Cr16W10C10 precursor mixed powders.

lead to severe ploughing plastic deformation and slight adhesive transfer.

In contrast the high-temperature worn surface morphologies of the laser clad γ/W_2C/TiC composite coating with Ni40Cr10W25C25 and Ni64Cr16W10C10 precursor mixed powders is smooth, without any serious grooves and plastic deformation features observable. However, much more adhesive transfer layer can be easily observed, as shown in Fig. 6(b) and more clearly in Fig. 6(c). EDS analysis results indicate that the white raised "small islands" area in Fig. 6(b) are enriched in Cr, Ni, Fe, Ti, and the large flat area in Fig. 6 (c) contains a large amount of Fe, Cr, Ni, little Ti, Al and minimum O. It implies that the formation of the white raised "little islands" area in Fig. 6(b) is primarily attributed to the adhesive transfer from the counterpart steel. At the same time, the existence of the little high-temperature wear debris (such as W_2C and TiC) detached from the coating could be detected. Slight oxidation-wear characteristic could also occur because of the presence of a little oxygen based on EDS analysis, which is evidenced by the blue color of the worn surface. The composition of the large flat area in Fig. 6(c) is much more close to that of the counterpart stainless steel, which demonstrates that it is formed mostly through adhesive transfer from the mating steel. The above analysis clearly indicates that after high-temperature sliding wear, compared with the original TiAl alloy, the laser clad composite coating demonstrates aggravated adhesive transfer and alleviated micro-cutting and scratching. As a result, the laser clad composite coatings exhibit increased high-temperature wear resistance than that of the original TiAl alloy when sliding on a metallic surface.

From the above high-temperature wear experiment results and the related deduction, it can be understood that the excellent high-temperature wear resistance is attributed to the following main causes. First there are large volume fraction of high hardness and high-temperature (at 600 °C) stability reinforced phases, such as α-W_2C and TiC, dispersed uniformly in the composite coating that provide the coating with excellent high-temperature abrasive wear resistance. The mating counterpart steel can hardly press into the coating to generate micro-cutting and can only slightly "scratching or rubbing" the coating through the mechanism of "mild abrasive wear or soft abrasive wear" in the softer matrix phase. A similar phenomenon was

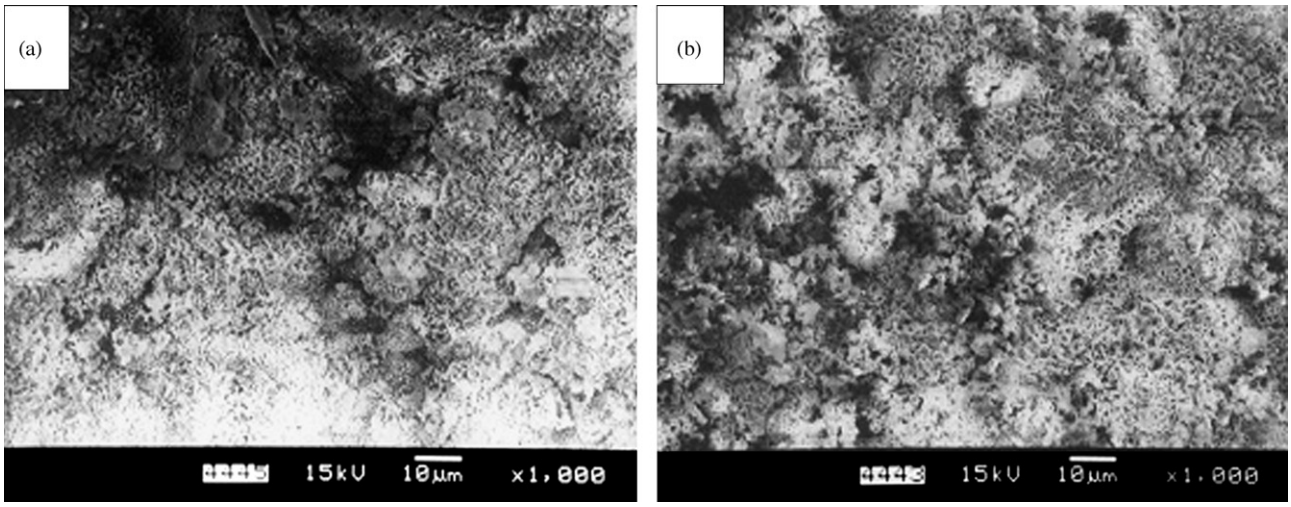

Fig. 7. Surface SEM images of the laser clad composite coatings with Ni40Cr10W25C25 (a) and Ni64Cr16W10C10 (b) precursor mixed powders after exposure at 1000 °C for 50 h.

also observed by Wang et al. [15], when ternary metal silicide Ti_2Ni_3Si/NiTi intermetallic coatings were fabricated on a 0.2% C low carbon steel and mated with the 0.45% C steel counterpart during room-temperature dry sliding wear process. Second, since the reinforced carbides are of unique covalent-dominant strong atomic bonds, it is very hard for them to generate plastic deformation and adhesion on the actual contacting surface of the slide-coupling metallic counterpart. The counterpart steel can only scrape the coating very slowly through the above-mentioned "slight scratching" method, thus imparts the coating excellent high-temperature adhesive wear resistance. Third, as the matrix of the laser clad coating, i.e., the ductile and tough γ nickel solid solution, can effectively release the stress concentration of the coating under high-temperature environment, the tendency of cracking and brittle delamination of the coating as a whole during the high-temperature wear process is decreased. Simultaneously, as the hardness and strength of the counterpart steel are all decreasing under high-temperature, the coating surface, which still possesses high hardness, can press into and cut the surface of the counterpart steel, making the steel surface generate serious plastic deformation and the formation of plastic flow thin films. Research results in literature [16] had mentioned the same phenomena. Afterwards, the plastic flow thin films transforms to the coupling coating's surface through adhesive transfer. Finally, large area of flat adhesive transfer layer are formed through the subsequently repeated grinding and wear process, as shown in Fig. 6(b and c). So, it is very clear that the mechanisms of the laser clad composite coating are mainly slight micro-cutting and serious adhesive transfer.

3.3. High-temperature oxidation resistance

The isothermal high-temperature oxidation resistance of the original TiAl alloy was studied in our previous work [8], since the preferential formation of the coarse bulky square rutile TiO_2 grains and the bulky and dispersive distribution on the top layer oxide scale [17,18], no compact protective oxide scale occurred, the oxide scales are brittle and relatively porous, so the original TiAl alloy shows inadequate high-temperature oxidation resistance after 50 h exposure at 1000 °C.

WC is also reported to possess good resistance against oxidation under 600 °C environment [9], the question of how about the isothermal oxidation resistance of the laser clad γ/W_2C/TiC composite coatings at 1000 °C is put forward. Unfortunately, the testing results showed that the weight gain per square millimeter of the laser clad composite coating with Ni64Cr16W10C10 is slightly more than that of the original TiAl alloy, but about 30% more than that of the original for the Ni40Cr10W25C25 coating.

In order to clarify the reasons for the decreased high-temperature oxidation resistance of the laser clad composite coatings, the surface images of the oxide layer on the laser coatings after exposure at 1000 °C for 50 h were photographed, as can be seen in Fig. 7(b) and more clearly in Fig. 7(a). Big cracks and even large area spallation and holes were formed, there could be the following possible explanations for this phenomenon. First, the limited oxidation temperature of the carbides in the composite coating, i.e., W_2C and TiC, is relatively low (far less than 1000 °C), the generation of CO and CO_2 during oxidation of W_2C leads to cracking in WO_3 owing to the force of the escaping gaseous species, large amount of brittle and porous TiO_2 oxide scale was formed as a result of the volatilization of tungsten oxides. Second, from the thermodynamic point of view, Ti diffuses much fast in TiO_2, for example, than that of Al in $A1_2O_3$, so the growing velocity of TiO_2 is much fast during the high-temperature oxidation conditions, the adherence between the formed oxide scales and the substrate is poor, large amount of penetrating big cracks were formed due to thermal and growing stresses during the period of long term high-temperature exposure, leading to spallation and even exfoliation of the oxide scale, this phenomenon was more evident for the Ni40Cr10W25C composite coating, whose W and C content is higher. Basu and Sarin [19] had studied the high-temperature oxidation behavior of WC–Co and found that the oxidation rate of WC–Co was almost negligible at 600 °C, but with a rapid increase in the oxidation rate with temperature, the

dominant phases were WO_3 with the long column structure and $CoWO_4$with the dispersed phase, the WO_3 formed during the initial stages of oxidation appears to gradually change from a very strong {0 0 1} texturing at 600 °C to a very weak {2 0 0} texturing at 800 °C. It has been also reported that WO_3 starts to evaporate under vacuum at 800 °C and the rate becomes significant at 850 °C [20]. These research results could provide some evidence and support to certain extent for our experiments and analyses, we can say that although laser cladding γ/W_2C/TiC composite coatings on TiAl alloy shows decreased high-temperature oxidation resistance at 1000 °C, it still possess good high-temperature sliding wear and oxidation resistance at and below 600 °C. From our previous works [8,21], the relative room-temperature wear resistance of the γ/W_2C/TiC composite coatings as against of the original TiAl alloy (as high as 5.7) is high than that of the γ/Cr_7C_3/TiC composite coatings (the highest is 1.90). Thus, when the service temperature of TiAl alloy tribological moving components is below 600 °C, it would be more beneficial to fabricate γ/W_2C/TiC composite coatings on TiAl alloys.

4. Conclusions

The microstructure, high-temperature dry sliding wear at 600 °C and isothermal oxidation at 1000 °C behaviors of the laser clad γ/W_2C/TiC composite coatings have been investigated. The composite coatings possess non-equilibrium solidified microstructure consisting of the α-W_2C, TiC and $M_{23}C_6$ hard carbides distributed in the tough γ nickel solid solution matrix. Mechanical tests show that the laser clad composite coatings exhibit high hardness, increased wear resistance under high-temperature sliding wear test conditions due to the higher hardness and stability of the reinforcing phases in the composite coating at 600 °C. The mechanisms are mainly slight micro-cutting and serious adhesive transfers, while the dominant high-temperature sliding wear mechanism of the original TiAl alloy demonstrates severe plastic deformation and slight adhesive transfer. The laser clad γ/W_2C/TiC composite coatings show decreased isothermal oxidation resistance at 1000 °C due to the formation of brittle and porous TiO_2 oxide scale as a result of the volatilization of tungsten oxides and large amount of penetrating cracks, leading to spallation and even exfoliation of the oxide scale. Nevertheless, laser clad γ/W_2C/TiC composite coatings is still a promising high-temperature wear resisting surface modification technique for TiAl alloy at or below 600 °C.

Acknowledgements

One of the authors, Xiu-Bo Liu, wishes to thank Professor Gang Yu, Dr. Hong-Wei Song and PhD student Ming Pang of the Laboratory for Laser Intelligent Manufacturing, Institute of Mechanics, Chinese Academy of Sciences, for their beneficial discussions.

References

[1] D.M. Dimiduk, Mater. Sci. Eng. A263 (1999) 281–288.
[2] Y.M. Kim, Acta Metall. Sin. 12 (4) (1999) 334–339.
[3] He Qiang Ye, Mater. Sci. Eng. A263 (1999) 289–295.
[4] Blackburn, M.J., Smith, M.P., 1989. Report WPDC-TR-89-4133, 1989.
[5] Y.G. Zhang, X.Y. Li, et al., Surf. Coat. Technol. 100–101 (1998) 214–218.
[6] M. Yoshihara, T. Suzuki, R. Tanaka, ISIJ Int. 31 (1991) 1201–1206.
[7] Y. Chen, H.M. Wang, Appl. Surf. Sci. 220 (2003) 186–192.
[8] X.-B. Liu, H.-M. Wang, Appl. Surf. Sci. 252 (2006) 5735–5744.
[9] B. Vamsi Krishna, V.N. Misra, P.S. Mukherjee, et al., Int. J. Refract. Met. Hard Mater. 20 (2002) 355–374.
[10] Sen Yang, Wenjin Liu, Minim Zhong, et al., Mater. Lett. 58 (2004) 2958–2962.
[11] J.J. Guo, B.S. Li, J.Z. Zhao, Trans. Nonferrous Met. Soc. China 5 (4) (1995) 142–145.
[12] A.H. Cottrell, Mater. Sci. Technol. 11 (3) (1995) 209–212.
[13] P. Wu, H.M. Du, X.L. Chen, et al., Wear 257 (2004) 142–147.
[14] J.A. Hawk, D.E. Alman, Mater. Sci. Eng. A239–240 (1997) 899–906.
[15] H.M. Wang, F. Cao, L.X. Cai, et al., Acta Mater. 51 (2003) 6319–6327.
[16] Y. Liu, H.M. Wang, Scripta Mater. 51 (2005) 1235–1240.
[17] Y.G. Zhao, W. Zhou, Q.D. Qin, et al., J. Alloys Compd. 391 (2005) 136–140.
[18] T. Izumi, T. Nishimoto, T. Nanta, Intermetallics 13 (2005) 615–619.
[19] S.N. Basu, V.K. Sarin, Mater. Sci. Eng. A209 (1996) 206–212.
[20] E.A. Gulbransen, W.S. Wysong, Technical Publication No. 2224, American Institute of Mining and Metallurgical Engineers, New York, NY, 1947.
[21] X.B. Liu, L.G. Yu, H.M. Wang, Chin. J. Nonferrous Met. 10 (6) (2000) 785–789.